Archival Report

Biological Psychiatry: Celebrating 50 Years

Chromodomain Y-like Protein–Mediated Histone Crotonylation Regulates Stress-Induced Depressive Behaviors

Yongqing Liu, Minghua Li, Minghua Fan, Yan Song, Huajing Yu, Xiaojie Zhi, Kuo Xiao, Shirong Lai, Jingliang Zhang, Xueqin Jin, Yongfeng Shang, Jing Liang, and Zhuo Huang

ABSTRACT

BACKGROUND: Major depressive disorder is a prevalent and life-threatening illness in modern society. The susceptibility to major depressive disorder is profoundly influenced by environmental factors, such as stressful lifestyle or traumatic events, which could impose maladaptive transcriptional program through epigenetic regulation. However, the underlying molecular mechanisms remain elusive. Here, we examined the role of histone crotonylation, a novel type of histone modification, and chromodomain Y-like protein (CDYL), a crotonyl-coenzyme A hydratase and histone methyllysine reader, in this process.

METHODS: We used chronic social defeat stress and microdefeat stress to examine the depressive behaviors. In addition, we combined procedures that diagnose behavioral strategy in male mice with histone extraction, viral-mediated CDYL manipulations, RNA sequencing, chromatin immunoprecipitation, Western blot, and messenger RNA quantification.

RESULTS: The results indicate that stress-susceptible rodents exhibit lower levels of histone crotonylation in the medial prefrontal cortex concurrent with selective upregulation of CDYL. Overexpression of CDYL in the prelimbic cortex, a subregion of the medial prefrontal cortex, increases microdefeat-induced social avoidance behaviors and anhedonia in mice. Conversely, knockdown of CDYL in the prelimbic cortex prevents chronic social defeat stress–induced depression-like behaviors. Mechanistically, we show that CDYL inhibits structural synaptic plasticity mainly by transcriptional repression of neuropeptide VGF nerve growth factor inducible, and this activity is dependent on its dual effect on histone crotonylation and H3K27 trimethylation on the *VGF* promoter.

CONCLUSIONS: Our results demonstrate that CDYL-mediated histone crotonylation plays a critical role in regulating stress-induced depression, providing a potential therapeutic target for major depressive disorder.

Keywords: CDYL, Dendritic spine, Depression, Histone crotonylation, Stress, VGF

https://doi.org/10.1016/j.biopsych.2018.11.025

Major depressive disorder (MDD) is one of the most prevalent mental disorders in modern society. The susceptibility to MDD is affected by both genetic variations and environmental factors such as stressful and traumatic life events. Adverse environmental insults could lead to altered neuronal circuits and brain reward function, posing the risk to trigger the onset of MDD. Maladaptive transcriptional programming in susceptible neurons contributes to the development of MDD. However, the underlying molecular mechanisms remain elusive (1–3).

One important way to transduce the ever-changing extracellular signals to intracellular effects is through dynamic and versatile protein posttranslational modifications (PTMs). In particular, reversible histone PTMs are important in regulating gene expression in eukaryotic cells. Several studies have investigated the role of histone acetylation and methylation of H3K4/9/27 (H3K4/9/27me) in neuronal diseases including depression (4,5). Recently, researchers have discovered a group of chemically diverse short-chain histone acylations, including formylation, propionylation, butyrylation, 2-hydroxyisobutyrylation, β-hydroxybutyrylation, crotonylation (Kcr), malonylation, succinylation, glutarylation, 4-pentynoylation, 3-phosphoglycerylation, palmitoylation, and myristoylation (6–10). However, the function of these modifications in terms of gene regulation is still in its infancy stage, and whether and how they play a role in neuronal diseases including depression have not been investigated.

Among these newly identified histone acylations, Kcr was previously shown to be associated with actively transcribed genes and play a role in spermatogenesis (8). The donor of crotonyl group is crotonyl-coenzyme A (CoA), which is a four-carbon acyl chain containing one double bond. It has been reported that classic acetyltransferase p300 can add histone Kcr (11), whereas histone deacetylase (HDAC) 1/2/3 and sirtuin

SEE COMMENTARY ON PAGE 616

ISSN: 0006-3223

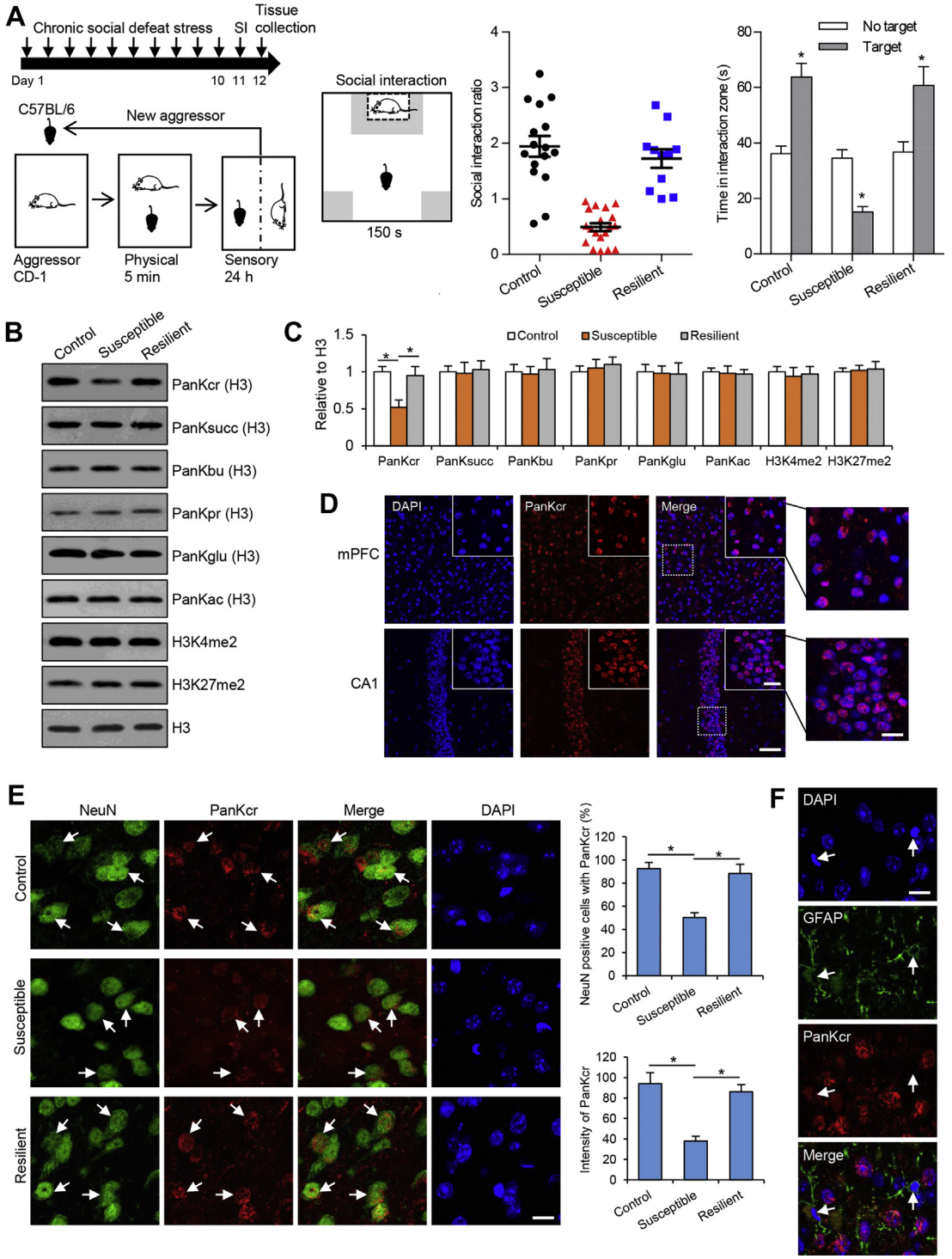

Figure 1. Chronic social defeat stress (CSDS) decreased histone crotonylation (Kcr) expression in the medial prefrontal cortex (mPFC) of susceptible mice. **(A)** Illustration of the CSDS procedures. A schematic diagram of CSDS and social interaction (SI) test (left) and distribution of interaction ratios (middle, right) for control, susceptible, and resilient mice after CSDS. Unpaired two-tailed Student's *t* test, $^{*}p < .05$. **(B)** Western blot assays showing histone Kcr was decreased in the mPFC in the 48 hours after CSDS. **(C)** Quantification of the Western blotting by normalizing the level of indicated protein to that of H3. $n = 3$, one-way analysis of variance with Bonferroni's test, $^{*}p < .05$. **(D)** Immunofluorescent staining indicating widely distribution of histone crotonylation in the mPFC and CA1 coronal sections. Scale bar = 50 μm (bottom row), 20 μm (top row), 8 μm (insets). **(E)** Immunofluorescence assays showing histone crotonylation was decreased in mPFC neurons in the 48 hours after CSDS. $n = 3$, one-way analysis of variance with Bonferroni's test, $^{*}p < .05$. Scale bar = 5 μm. **(F)** Immunofluorescence assays showing that histone crotonylation was not detected in glial cells. Scale bar = 5 μm. Data are presented as mean ± SEM. GFAP, glial fibrillary acidic protein.

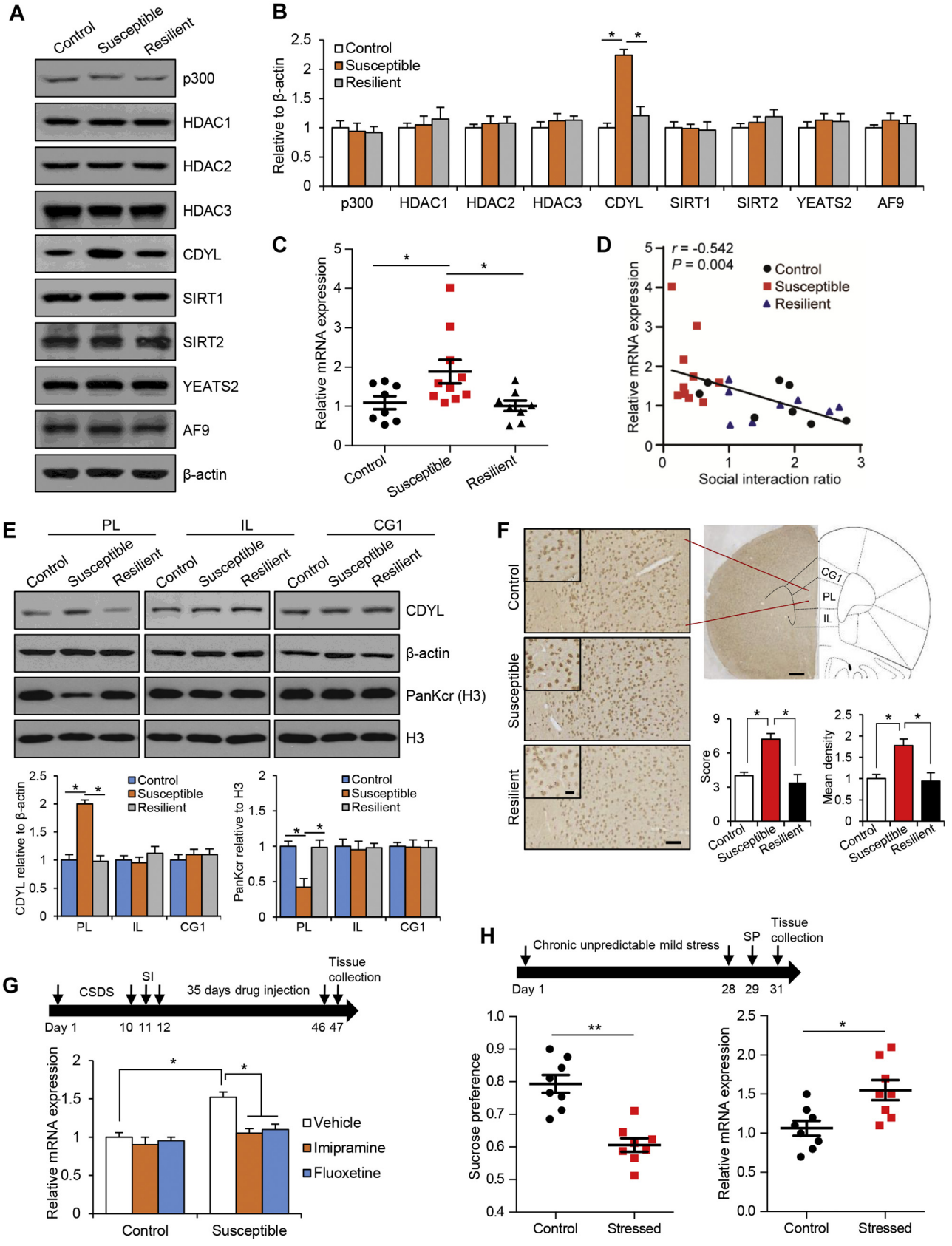
A
Control
Susceptible
Resilient
p300
HDAC1
HDAC2
HDAC3
CDYL
SIRT1
SIRT2
YEATS2
AF9
β-actin
B
Relative to β-actin
Control
Susceptible
Resilient
p300
HDAC1
HDAC2
HDAC3
CDYL
SIRT1
SIRT2
YEATS2
AF9
C
Relative mRNA expression
Control
Susceptible
Resilient
D
r = -0.542
P = 0.004
Relative mRNA expression
Social interaction ratio
Control
Susceptible
Resilient
E
PL
IL
CG1
Control
Susceptible
Resilient
CDYL
β-actin
PanKcr (H3)
H3
CDYL relative to β-actin
PanKcr relative to H3
F
Control
Susceptible
Resilient
CG1
PL
IL
Score
Mean density
G
CSDS
SI
35 days drug injection
Tissue collection
Day 1
10 11 12
46 47
Relative mRNA expression
Vehicle
Imipramine
Fluoxetine
Control
Susceptible
H
Chronic unpredictable mild stress
SP
Tissue collection
Day 1
28 29 31
Sucrose preference
Relative mRNA expression
Control
Stressed

1/2/3 can remove Kcr (12–14). In addition, the YEATS family proteins YEATS2 and AF9 were identified as readers of histone Kcr (15,16). Interestingly, we recently showed that chromodomain Y-like protein (CDYL), a transcriptional corepressor and histone H3K9/27 methyllysine reader (17–20), acts as a crotonyl-CoA hydratase and negatively regulates histone Kcr (21). Here, we report that CDYL-mediated histone crotonylation in the medial prefrontal cortex (mPFC) regulates stress-induced depressive behaviors in rodents. Our study provides new insight to link histone PTMs to stress-induced depression and suggests CDYL as a potential therapeutic target for MDD.

METHODS AND MATERIALS

Animals

Male adult Sprague Dawley rats (6–8 weeks old), C57BL/6 male mice (6–8 weeks old), and 6- to 8-month-old CD-1 male retired breeder mice were obtained from Charles River Laboratories (Beijing, China). All animals were housed on a 12-hour light/dark cycle with ad libitum access to food and water and acclimated to the facility for 1 week before any experiment. All experimental procedures were approved by Peking University Institutional Animal Care and Use Committee. Every effort was made to minimize animal suffering and the number of animals used. The experimenters were blinded to viral treatment or drug treatment condition during behavioral testing. The experimental procedures were performed in a double-blind manner.

Social Defeat Stress and Social Interaction Testing

Chronic social defeat stress (CSDS) was performed according to previously described protocols (22). Briefly, experimental C57BL/6 mice were physically defeated by a novel CD-1 aggressor for 5 min/day for up to 10 days. After each physical interaction, C57BL/6 mice were kept in one side of the cages divided by a transparent, perforated partition, sensory contacting with CD-1 mice on the other side for 24 hours. Control C57BL/6 mice were pair-housed in the cage with one mouse on each side of the perforated divider. All control mice that were placed with the control group were changed daily. On day 11, defeated and control animals were subjected to the social interaction test. To measure increased susceptibility to stress, we used a subthreshold "microdefeat," as previously described (23,24). In the microdefeat protocol, C57BL/6 mice were exposed to a novel CD-1 aggressor for three consecutive 5-minute defeat sessions, each separated by 15 minutes; 24 hours later, mice were subjected to the social interaction test. More details are provided in the Supplement.

Chronic Unpredictable Mild Stress

Chronic unpredictable mild stress was performed as previously described (25,26). Male adult rats were age- and weight-matched before commencement of chronic unpredictable mild stress procedures. Rats were subjected to a sequence of 11 stressors during the course of 28 days. All stressors were randomly interspersed throughout the stress period. The detailed chronic unpredictable mild stress procedure is in Supplemental Table S1.

RNA Sequencing

Total messenger RNA (mRNA) was extracted from prelimbic cortex (PL) tissues of susceptible or control mice; or extracted from PL tissues of adeno-associated virus (AAV)–CDYL AAV-CDYL or AAV–green fluorescent protein (GFP)–injected mice. High-throughput RNA sequencing (RNA-seq) was performed by Illumina HiSeq 2500 (Illumina, San Diego, CA) at CapitalBio Corporation (Beijing, China). The raw sequencing data were aligned to the mouse preference genome (GRCm38, mm10). We used a p value $< .05$ and fold changes cutoff as $|\log_2 \text{ratio}| \geq 0.5$ for detection of differentially expressed genes in the RNA-seq analysis. Pathway analysis (q value $< .05$) against these downregulated genes was conducted using DAVID tools (https://david.ncifcrf.gov/) and the analyzed results are provided in Supplemental Table S3. The RNA-seq data have been deposited in the Gene Expression Omnibus (accession number GSE120293).

Chromatin Immunoprecipitation and Quantitative Chromatin Immunoprecipitation

Chromatin immunoprecipitation (ChIP) experiments were performed according to the procedure described previously (20,27). Quantification of the precipitated DNA fragments were performed with real-time polymerase chain reaction (PCR) using primers listed in Supplemental Table S4. More details are provided in the Supplement.

Figure 2. Chronic social defeat stress (CSDS) increased chromodomain Y-like protein (CDYL) expression in the prelimbic cortex (PL) of susceptible but not resilient mice. **(A)** Western blotting and **(B)** quantification showing CDYL was increased in the medial prefrontal cortex (mPFC) of susceptible mice in the 48 hours after CSDS. $n = 3$, one-way analysis of variance (ANOVA) with Bonferroni's test, $^*p < .05$. **(C)** Quantitative real-time polymerase chain reaction analysis indicating that *Cdyl* messenger RNA (mRNA) was increased in the mPFC of susceptible mice in the 48 hours after CSDS. $n = 8$–10 mice per group, one-way ANOVA with Bonferroni's test, $^*p < .05$. **(D)** Correlation of *Cdyl* mRNA level in the mPFC with social interaction (SI) ratio (Pearson correlation, $n = 8$–10 mice per group). mPFC tissues were obtained in the 48 hours after CSDS. **(E)** Representative Western blotting and quantification of CDYL protein and histone crotonylation expression in the prelimbic cortex (PL), infralimbic cortex (IL), and cingulate cortex area 1 (CG1) after CSDS. $n = 4$, one-way ANOVA with Bonferroni's test, $^*p < .05$. **(F)** Immunohistochemical staining showing increased expression of CDYL protein in the PL of susceptible mice. $n = 4$ mice per group, one-way ANOVA with Bonferroni's test, $^*p < .05$. Scale bar = 10 μm (left), 35 μm (middle), 0.15 mm (right). **(G)** *Cdyl* mRNA level after 35 days of imipramine, fluoxetine (20 mg/kg/day, intraperitoneal), or vehicle injection in previously susceptible mice showing that imipramine and fluoxetine can reverse the upregulation of *Cdyl* expression in the PL. $n = 4$–6 mice per group, two-way ANOVA with Bonferroni's test, $^*p < .05$. **(H)** Stressed rats decreased sucrose preference (SP) after chronic unpredictable mild stress when compared with control rats (left). Quantitative real-time polymerase chain reaction analysis indicating that *Cdyl* mRNA expression was increased in the PL of stressed rats after chronic unpredictable mild stress (right). $n = 8$ rats per group, unpaired two-tailed Student's t test, $^*p < .05$, $^{**}p < .01$. Data are presented as mean ± SEM. HDAC, histone deacetylase; SIRT, sirtuin.

Biological Psychiatry: Celebrating 50 Years

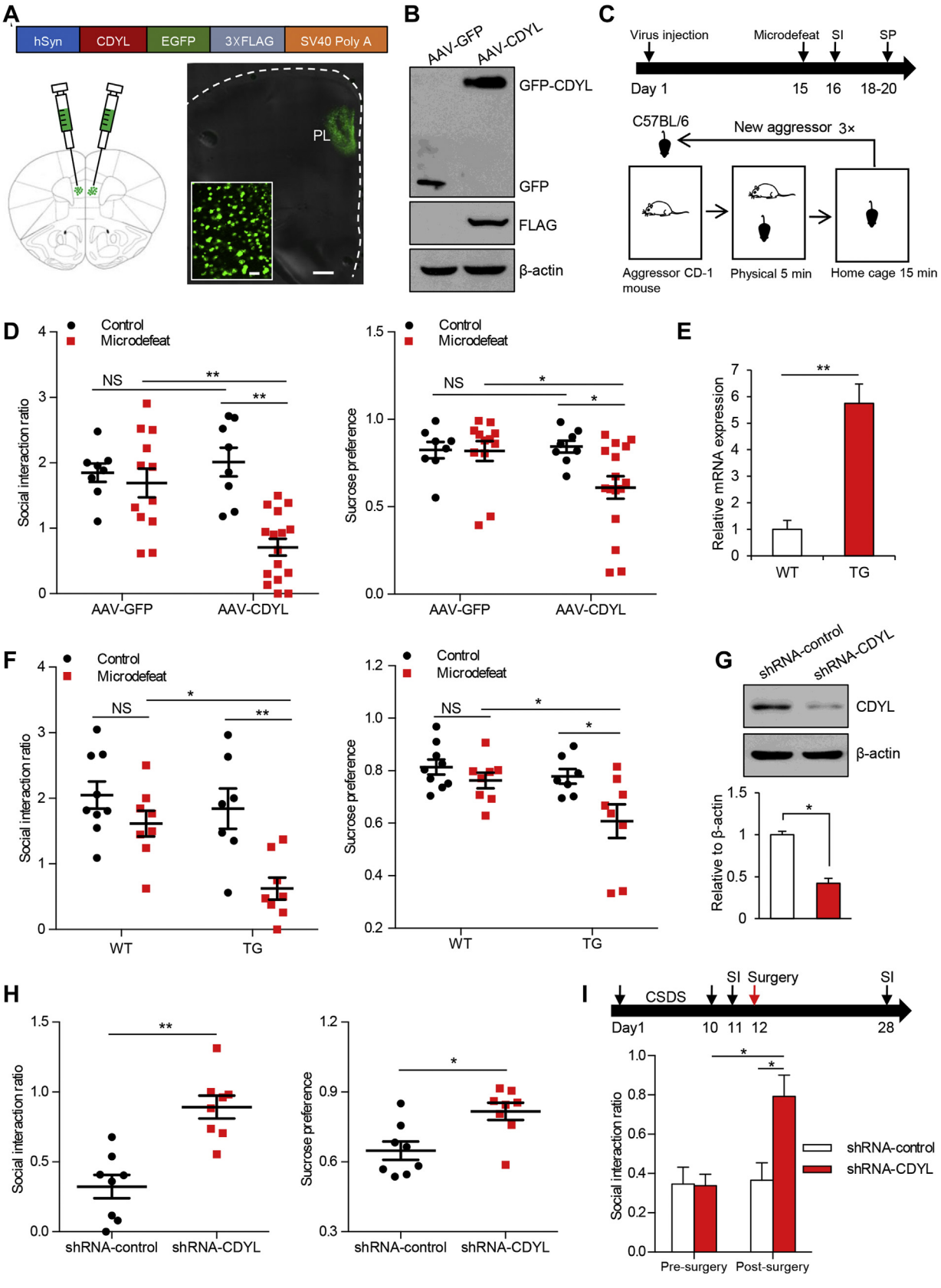

Statistical Analysis

For in vivo experiments, the animals were distributed into various treatment groups randomly. For in vitro experiments, the cells were evenly suspended and then randomly distributed in each well tested. Comparisons between two groups were made using Student's paired or unpaired two-tailed *t* test as appropriate. Comparisons among three or more groups were made using one- or two-way analysis of variance followed by Bonferroni's multiple-comparisons test. The details of two-way analysis of variance are provided in the Supplemental Table S5. All experiments and analysis of data were performed in a blinded manner by investigators who were unaware of the genotype or manipulation. Statistical analyses were performed using GraphPad Prism 6 (GraphPad Software, La Jolla, CA) and SPSS 13.0 software (SPSS Inc., Chicago, IL). Before statistical analysis, variation within each group of data and the assumptions of the tests were checked. All data are presented as mean ± SEM.

Methods are described in more detail in the Supplement.

RESULTS

Histone Kcr Is Decreased in the mPFC After CSDS

The PFC controls higher-level "executive" functions and is intimately involved in MDD (28–30). C57BL/6 adult male mice were subjected to CSDS, an ethologically validated model of depression (22), and experimental mice were classified as susceptible or resilient based on their social interaction time (Figure 1A). Forty-eight hours after the last social defeat, histones were acid-extracted from mPFC, and the levels of a panel of histone acylations were examined by Western blotting. CSDS led to significant decrease of histone Kcr in susceptible mice but not in resilient mice, whereas no changes of other histone acylations including propionylation, butyrylation, succinylation, glutarylation, acetylation, H3K4me2, and H3K27me2 were observed in either susceptible or resilient mice (Figure 1B, C). Downregulation of histone Kcr or other histone acylations was not observed in susceptible mice in the hippocampus, another brain region implicated in depression (Supplemental Figure S1A, B). Immunofluorescence assays showed widely distributed histone Kcr throughout mouse brain, with higher levels in the mPFC and hippocampal CA1 (Figure 1D and Supplemental Figure S1C, D). Within the mPFC, neurons generally exhibited higher levels of histone Kcr than glial cells (Figure 1E, F), and decreased histone Kcr was observed in susceptible mice after CSDS (Figure 1E), supporting a role of this modification in mPFC-mediated stress-induced depression.

Crotonyl-CoA Hydratase CDYL Is Selectively Upregulated in the PL of the mPFC After CSDS

We next examined the expression levels of Kcr-associated regulators to understand the mechanisms of CSDS-induced alteration of histone Kcr. Selective upregulation of only CDYL, a crotonyl-CoA hydratase and negative Kcr regulator, was found in the mPFC of susceptible mice (Figure 2A, B). *Cdyl* mRNA expression in the mPFC was strongly correlated with social avoidance behavior of susceptible mice (Figure 2C, D). CSDS did not cause changes of CDYL protein levels in the nucleus accumbens (NAc) in both susceptible and resilient mice (Supplemental Figure S2A, B), whereas CDYL protein levels were increased in both groups in the dorsal hippocampus (Supplemental Figure S2C, D). These data together suggest that the mPFC is the region where CDYL-mediated Kcr regulation could play a role in CSDS.

We further bilaterally obtained three mPFC subregions, including the cingulate cortex area 1, PL, and infralimbic cortex, and performed Western blots. Compared to resilient mice of CSDS, susceptible mice exhibited increased CDYL expression and decreased histone Kcr only in the PL and not in cingulate cortex area 1 or the infralimbic cortex (Figure 2E). Selective upregulation of CDYL in the PL was also confirmed by immunohistochemical staining (Figure 2F). Upregulated *Cdyl* expression in the PL could last for more than 1 month, which could be partially reversed by chronic antidepressant treatment with imipramine or fluoxetine once daily for 35 days (Figure 2G). Upregulation of *Cdyl* expression in the PL was also observed after 28 days of chronic unpredictable mild stress in male rats (Supplemental Table S1, Figure 2H). Knockdown of CDYL in the PL with its specific short hairpin RNA (shRNA) selectively increased the level of histone Kcr but not the level of other acylations (Supplemental Figure S2E, F), suggesting that CDYL-mediated Kcr regulation in the PL is involved in chronic stress–induced depression.

CDYL in the PL Promotes Stress-Induced Depression-like Behaviors

To directly test whether upregulation of CDYL is a driver to stress susceptibility, we performed gain-of-function experiments by

Figure 3. Chromodomain Y-like protein (CDYL) expression in the prelimbic cortex (PL) controls stress-induced depression-like behaviors. **(A)** Expression of adeno-associated viruses (AAVs) in 14 days after infecting the mouse PL area. Scale bar = 10 μm (left), 0.2 mm (right). **(B)** Western blotting analysis of CDYL protein expression. The PL region of mice was injected with empty vector viruses or FLAG-green fluorescent protein (GFP)-CDYL viruses. Western blotting was performed with antibodies against FLAG, GFP, or β-actin. **(C)** Schematic of the microdefeat stress protocols detailing the timing for virus infection and behavioral testing. **(D)** AAV-CDYL–injected mice decreased social interaction (SI) ratio (left) and sucrose preference (SP) (right) after microdefeat stress when compared with their respective control mice. n = 8–16 mice per group, two-way analysis of variance with Bonferroni's test, $^{*}p < .05$, $^{**}p < .01$. **(E)** Examination of *Cdyl* expression in the PL of the transgenic (TG) mice by quantitative real-time polymerase chain reaction assays. n = 3, unpaired two-tailed Student's t test, $^{**}p < .01$. **(F)** TG mice overexpressing CDYL decreased SI ratio (left) and SP (right) after microdefeat stress when compared with the respective control mice. n = 7–9 mice per group, two-way analysis of variance with Bonferroni's test, $^{*}p < .05$, $^{**}p < .01$. **(G)** Western blotting showing that CDYL was significantly reduced after short hairpin RNA (shRNA)-CDYL lentivirus injection into mice PL area for 14 days (upper). Quantification was done by normalizing the level of CDYL to that of β-actin (bottom). n = 3, unpaired two-tailed Student's t test, $^{*}p < .05$. **(H)** CDYL knockdown in the PL increased SI ratio (left) and SP (right) after CSDS. n = 8 mice per group, unpaired two-tailed Student's t test, $^{*}p < .05$, $^{**}p < .01$. **(I)** CDYL knockdown in previously susceptible mice could reverse the social avoidance behaviors. n = 9 mice per group, two-way analysis of variance with Bonferroni's test, $^{*}p < .05$. Data are presented as mean ± SEM. EGFP, enhanced green fluorescent protein; NS, not significant; WT, wild-type.

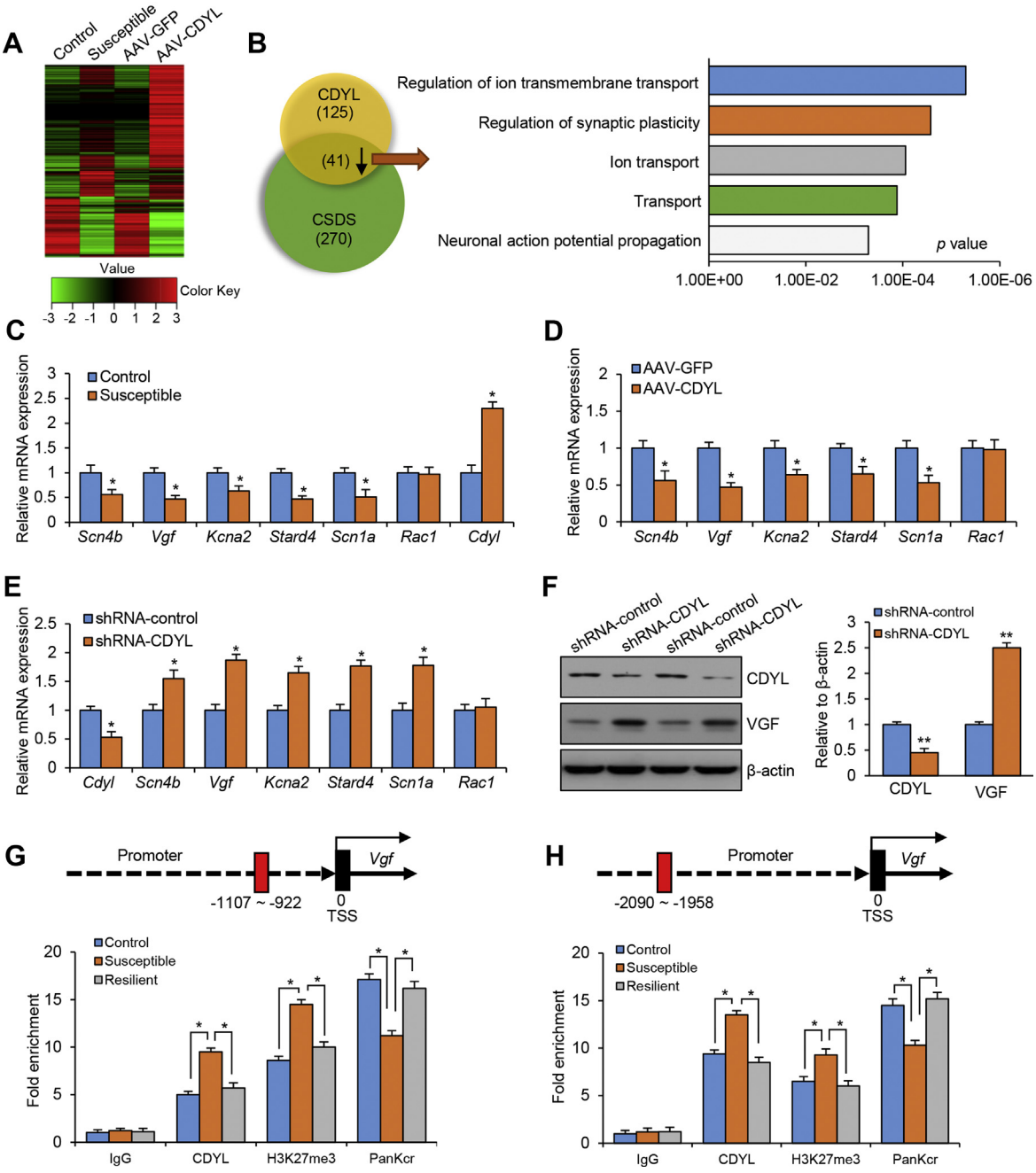

Figure 4. Genome-wide identification of chromodomain Y-like protein (CDYL)– and chronic social defeat stress (CSDS)–coregulated genes in the mouse prelimbic cortex (PL). **(A)** PL tissues were obtained from control or susceptible mice after CSDS and from mice infected with adeno-associated viruses (AAVs) containing CDYL or green fluorescent protein (GFP) for 14 days, followed by RNA extraction and deep sequencing. Heat maps showing up- or downregulated genes indicated by red or green color key, respectively. **(B)** Venn diagram of overlapping genes regulated by CDYL and CSDS in the mouse PL (left) and clustering of the 41 overlapping downregulated genes of CDYL and CSDS into biological process ontology using DAVID tools (right). Detailed ontology information is provided in Supplemental Table S3. **(C–E)** Quantitative real-time polymerase chain reaction analysis measuring the messenger RNA (mRNA) levels of indicated genes. Tissues were obtained from the PL of **(C)** control or susceptible mice, **(D)** mice injected with AAVs containing CDYL or GFP for 14 days, and **(E)** mice infected with lentiviruses containing CDYL short hairpin RNA (shRNA) or nonsilencing shRNA for 14 days. Levels of mRNA were normalized against that of *Gapdh*. $n = 4$ mice per group, unpaired two-tailed Student's *t* test, $^{*}p < .05$, $^{**}p < .01$. **(F)** Western blotting demonstrating knockdown of CDYL increased VGF nerve growth factor inducible (VGF) expression. Quantification was done by normalizing the level of CDYL to that of β-actin. PL tissues were obtained from mice infected with lentiviruses containing CDYL shRNA or nonsilencing shRNA for 14 days. $n = 3$, unpaired two-tailed Student's *t* test, $^{**}p < .01$. **(G, H)** Mouse PL tissues were obtained from control, susceptible, and resilient mice after CSDS. Chromatin immunoprecipitation experiments were performed using the indicated antibodies. Real-time polymerase chain reaction assays were performed for the measurement. Profiles of CDYL, H3K27me3, and PanKcr along the mouse *Vgf* promoter in **(G)** ~1000 bp and **(H)** ~2000 bp upstream of the transcription start site (TSS). $n = 3$, one-way analysis of variance with Bonferroni's test, $^{*}p < .05$. Data are presented as mean ± SEM. IgG, immunoglobulin G.

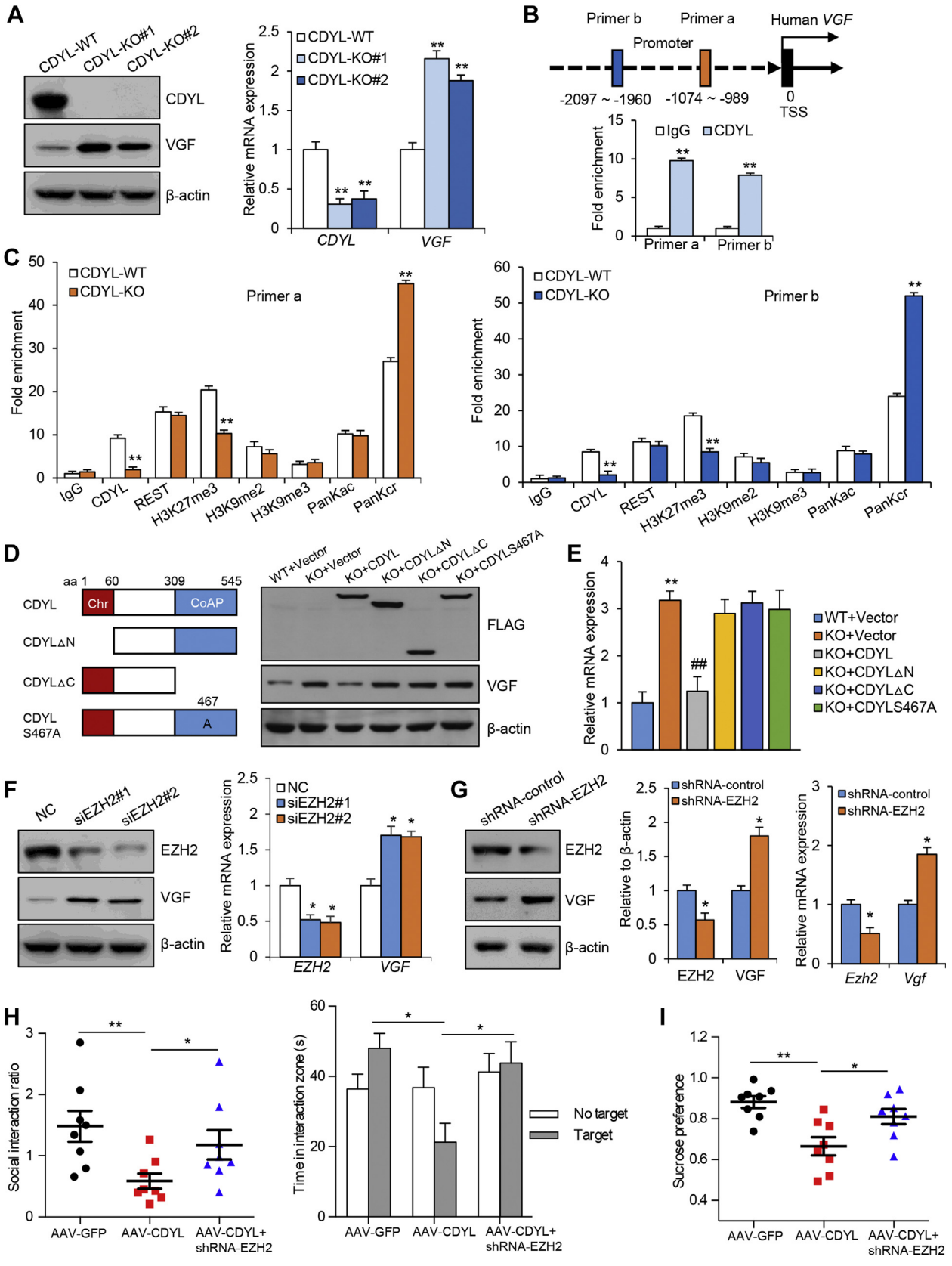
A
CDYL-WT
CDYL-KO#1
CDYL-KO#2
CDYL
VGF
β-actin
Relative mRNA expression
CDYL-WT
CDYL-KO#1
CDYL-KO#2
CDYL
VGF
B
Primer b
Primer a
Human VGF
Promoter
-2097 ~ -1960
-1074 ~ -989
0
TSS
Fold enrichment
IgG
CDYL
Primer a
Primer b
C
CDYL-WT
CDYL-KO
Primer a
Primer b
Fold enrichment
IgG
CDYL
REST
H3K27me3
H3K9me2
H3K9me3
PanKac
PanKcr
D
aa 1
60
309
545
CDYL
Chr
CoAP
CDYLΔN
CDYLΔC
467
CDYL S467A
A
WT+Vector
KO+Vector
KO+CDYL
KO+CDYLΔN
KO+CDYLΔC
KO+CDYLS467A
FLAG
VGF
β-actin
E
Relative mRNA expression
WT+Vector
KO+Vector
KO+CDYL
KO+CDYLΔN
KO+CDYLΔC
KO+CDYLS467A
F
NC
siEZH2#1
siEZH2#2
EZH2
VGF
β-actin
Relative mRNA expression
NC
siEZH2#1
siEZH2#2
EZH2
VGF
G
shRNA-control
shRNA-EZH2
EZH2
VGF
β-actin
Relative to β-actin
shRNA-control
shRNA-EZH2
EZH2
VGF
Relative mRNA expression
shRNA-control
shRNA-EZH2
Ezh2
Vgf
H
Social interaction ratio
AAV-GFP
AAV-CDYL
AAV-CDYL+ shRNA-EZH2
Time in interaction zone (s)
No target
Target
AAV-GFP
AAV-CDYL
AAV-CDYL+ shRNA-EZH2
I
Sucrose preference
AAV-GFP
AAV-CDYL
AAV-CDYL+ shRNA-EZH2

injecting AAVs carrying control or CDYL-GFP to the PL of adult male mice (Figure 3A, B). The susceptibility to stress of these animals was examined using a subthreshold social defeat paradigm known as microdefeat (Figure 3C), which does not cause any social avoidance or anhedonia in normal mice and thus is suitable to reveal prosusceptibility factors (31). Compared with control mice, overexpression of CDYL in the PL did not cause obvious depression-like behaviors before a microdefeat, whereas these mice exhibited increased social avoidance and decreased sucrose consumption after a microdefeat (Figure 3D). However, overexpression of CDYL in the infralimbic cortex did not affect stress-induced social avoidance (Supplemental Figure S3), indicating that the PL is the main region where CDYL plays a prodepressant role. The prodepressant function of CDYL was also confirmed in *Cdyl* transgenic mice (20) (Figure 3E), in which microdefeat induced significantly increased social avoidance behavior and decreased sucrose consumption compared with their wild-type littermates (Figure 3F). Together, these data suggest overexpression of CDYL in the PL promotes stress-induced depression in mice.

We next performed loss-of-function experiments in which we injected lentiviruses carrying control or CDYL-shRNA-GFP to the mouse PL region (Figure 3G). In accordance with the overexpression experiments, loss of CDYL expression had no effect on depression-like behaviors before CSDS (Supplemental Figure S4A–C), whereas increased social interaction and sucrose preference were observed in CDYL-shRNA–injected mice after CSDS (Figure 3H). The locomotor activity was not affected by either knockdown or overexpression of CDYL in the PL (Supplemental Figure S4D–H). In addition, we injected control or CDYL-shRNA lentiviruses in the PL of susceptible mice after CSDS. While control groups continued to display social avoidance behavior 2 weeks after the injection, this symptom was relieved in those that received CDYL-shRNA (Figure 3I). Together, we demonstrate that upregulation of CDYL in the PL is necessary and causal for susceptibility to depression in mice.

Comparative RNA-seq Reveals Transcriptional Targets of CDYL in the PL

To find the downstream targets of CDYL in mediating susceptibility to depression, RNA-seq was performed with PL tissues of adult mice infected with AAV-GFP or AAV-CDYL, as well as with PL tissues of control or susceptible mice exposed to CSDS. A cutoff with p value $< .05$ and $|\log_2 \text{ratio}| \geq 0.5$ was used to identify differentially expressed genes (Figure 4A). Because CDYL mainly acts as a transcription repressor, we focused on gene downregulation, as these genes are more likely to be direct targets of CDYL. Overexpression of CDYL in the PL caused downregulation of 166 genes, whereas CSDS caused downregulation of 311 genes in susceptible mice. Forty-one genes were downregulated in both groups (susceptible and AAV-CDYL–injected mice), which were classified into various signaling pathways using Kyoto Encyclopedia of Genes and Genomes analysis with a cutoff with q value $< .05$ (Figure 4B). The RNA-seq results in each classified pathway were validated at individual gene level by quantitative real-time PCR with selected genes, such as *Scn4b*, *Vgf*, *Kcna2*, *Stard4*, and *Scn1a* (Figure 4C, D). Injection of CDYL-shRNA lentiviruses to the mouse PL led to upregulation of these genes (Figure 4E), whereas the expression of a control gene *Rac1* was not altered in any of the above conditions (24) (Figure 4C–E).

CDYL Inhibits VGF Nerve Growth Factor Inducible Transcription by Its Dual Function on Histone Kcr and H3K27me3 on the Gene Promoter

Among the above RNA-seq–identified CDYL target genes, we paid special attention to *Vgf*, a neuropeptide that has been found to be downregulated in MDD patients and could induce an antidepressant response in mice (32–34). Upregulation of VGF nerve growth factor inducible (VGF) in CDYL-shRNA–injected PL tissues was confirmed by Western blotting (Figure 4F), whereas overexpression of CDYL in the PL led to decreased VGF expression (Supplemental Figure S5A). Consistent with our previous ChIP sequencing assay (20), robust binding of CDYL on the *Vgf* promoter was found by ChIP-quantitative PCR, and the enrichment of CDYL was significantly increased in susceptible mice upon CSDS, concomitant with significantly increased H3K27me3 and decreased histone Kcr (Figure 4G, H). We next used previously generated CDYL-knockout (KO) human SH-SY5Y cell lines (20) to examine the mechanism of CDYL-regulated VGF expression. As expected, significant upregulation of VGF was observed upon KO of CDYL in cells (Figure 5A). ChIP-quantitative PCR revealed strong enrichment of CDYL on *Vgf* promoter in wild-type SY5Y cells (Figure 5B), whereas such enrichment was diminished in CDYL-KO cells (Figure 5C). Significantly, increased enrichment of histone Kcr and decreased enrichment of H3K27me3 on *VGF* promoter were found in CDYL-KO cells, whereas the enrichment

Figure 5. Transcriptional repression of VGF nerve growth factor inducible (VGF) by chromodomain Y-like protein (CDYL). **(A)** Western blotting and real-time polymerase chain reaction (PCR) assays confirming the elimination of CDYL in human SH-SY5Y cells led to increased VGF expression. CDYL-knockout 1 (KO#1) were used for the subsequent functional studies. $n = 3$, unpaired two-tailed Student's t test, $^{**}p < .01$. **(B)** Quantitative chromatin immunoprecipitation assays were performed in SH-SY5Y cells with primer pairs specific to indicated regions. CDYL was strongly enriched in the human *VGF* promoter at ~1000 bp (primer a) and ~2000 bp (primer b) upstream of the transcription start site (TSS). $n = 3$, unpaired two-tailed Student's t test, $^{**}p < .01$. **(C)** Depletion of CDYL resulted in decreased regional enrichment of H3K27me3 and increased regional enrichment of histone crotonylation in the *VGF* promoter. Lysates from CDYL-KO cells were collected, and chromatin immunoprecipitation–quantitative PCR experiments were performed using the indicated antibodies. $n = 3$, unpaired two-tailed Student's t test, $^{**}p < .01$. **(D, E)** CDYL-KO SH-SY5Y cells were transfected with CDYL, CDYLΔN, CDYLΔC, or CDYLS467A. The expression of VGF was analyzed by **(D)** Western blotting and **(E)** quantitative real-time PCR. $n = 3$, unpaired two-tailed Student's t test, $^{**}p < .01$ vs. wild-type (WT) + Vector; $^{\#\#}p < .01$ vs. KO + Vector. Western blotting and real-time PCR indicating knockdown of EZH2 in **(F)** SH-SY5Y cells and **(G)** the mouse prelimbic cortex increased VGF expression. $n = 3$, unpaired two-tailed Student's t test, $^{*}p < .05$. Knockdown of EZH2 improved **(H)** social interaction and **(I)** sucrose preference reduction in adeno-associated virus (AAV)–CDYL–injected mice after microdefeat stress. $n = 8$ mice per group, one- or two-way analysis of variance with Bonferroni's test, $^{*}p < .05$, $^{**}p < .01$. Data are presented as mean ± SEM. Chr, chromodomain; CoAP, coenzyme A pocket; GFP, green fluorescent protein; IgG, immunoglobulin G; mRNA, messenger RNA; NC, normal control; REST, RE1-silencing transcription factor; shRNA, short hairpin RNA; siEZH2, small interfering RNA for EZH2.

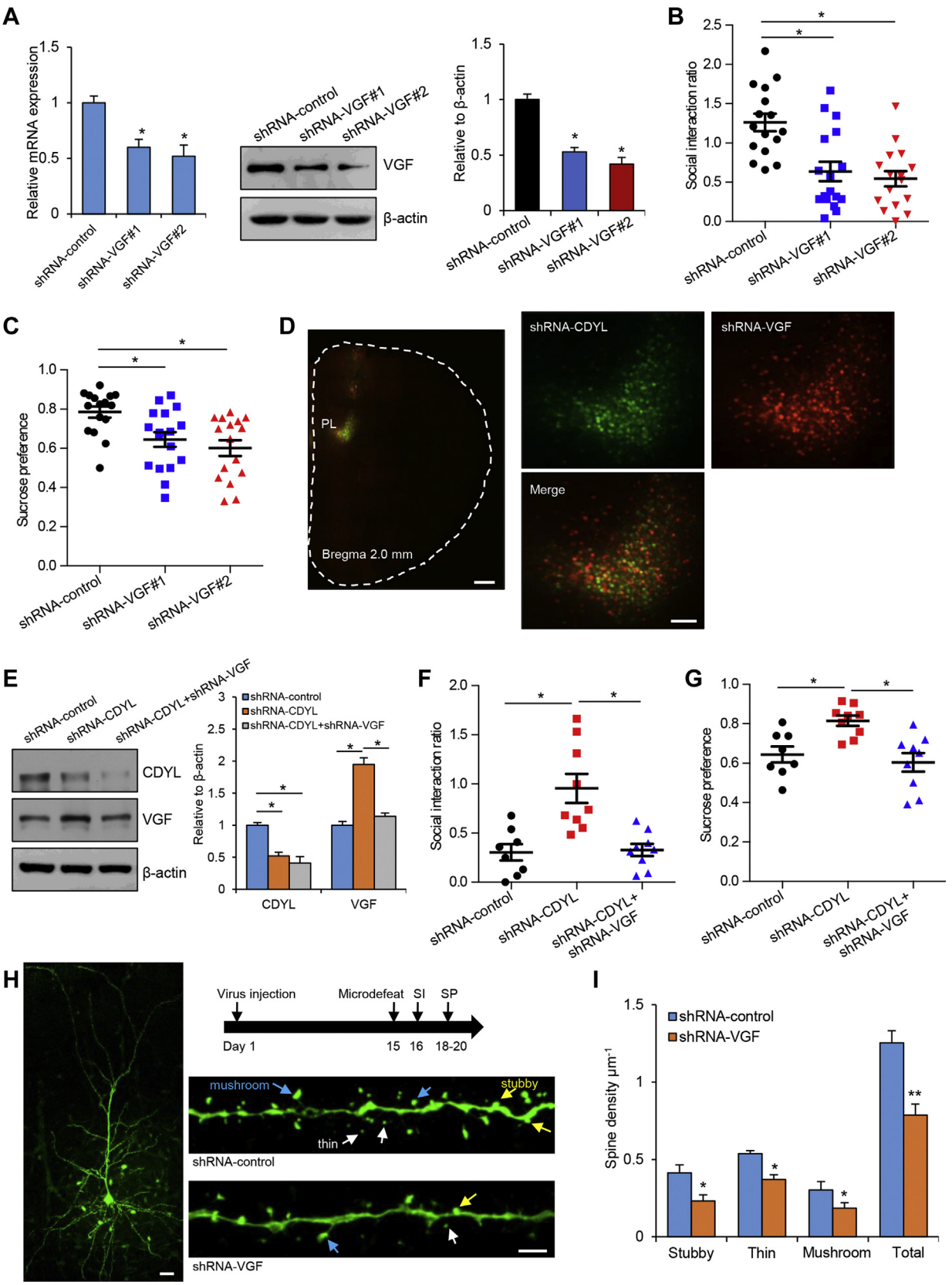
A
Relative mRNA expression
shRNA-control
shRNA-VGF#1
shRNA-VGF#2
VGF
β-actin
Relative to β-actin
B
Social interaction ratio
C
Sucrose preference
D
PL
Bregma 2.0 mm
shRNA-CDYL
shRNA-VGF
Merge
E
CDYL
shRNA-CDYL+shRNA-VGF
F
G
H
Virus injection
Microdefeat
SI
SP
Day 1
15
16
18-20
mushroom
stubby
thin
I
Spine density μm⁻¹
Stubby
Thin
Mushroom
Total

of H3K9me2/3 and histone acetylation was not changed (Figure 5C).

To further understand the mechanism of CDYL-mediated regulation of VGF expression, we performed rescue experiments, in which we overexpressed wild-type CDYL or CDYLΔN, CDYLΔC, or CDYLS467A mutants in CDYL-KO SY5Y cells. These mutants were used because we previously showed both the N-terminal chromodomain and the C-terminal coenzyme A pocket (CoAP) domain of CDYL are required for the negative regulation on histone Kcr, and CDYLS467A is defective of CoA binding and thus could not act on crotonyl-CoA and regulate histone Kcr (21). As shown by both Western blotting and quantitative real-time PCR, overexpression of only the wild-type CDYL and not the mutants reduced VGF expression in CDYL-KO cells (Figure 5D, E), supporting that the crotonyl-CoA hydratase activity of CDYL is critical to repress VGF expression. We previously established a coordinate function of CDYL with the H3K27 methyltransferase EZH2 in gene repression (18,20). Consistently, knockdown of EZH2 in either SH-SY5Y cells or the mouse PL led to significant upregulation of VGF (Figure 5F, G). As a control, knockdown of H3K9 methyltransferase G9a with specific small interfering RNAs in SH-SY5Y cells did not alter VGF expression (Supplemental Figure S5B, C). In addition, coinjection of shRNA-EZH2 with AAV-CDYL viruses in the mouse PL largely alleviated CDYL-mediated stress-induced depression (Figure 5H, I). Collectively, the above data demonstrate that CDYL inhibits VGF transcription by its dual effect on histone Kcr and H3K27me3 on the gene promoter.

VGF Is Required for CDYL-Mediated Stress-Induced Depression

We next examined whether VGF is required for CDYL-mediated regulation on depression-like behaviors. Injection of VGF-shRNA lentiviruses to the mouse PL region led to significantly increased social avoidance and anhedonia upon microdefeat treatment (Figure 6A–C), consistent with previously reported antidepressant-like effects of VGF (32,35). Coinjection of lentiviruses carrying VGF-shRNA-mCherry and lentiviruses carrying CDYL-shRNA-GFP to the mouse PL counteracted CDYL knockdown–induced VGF upregulation (Figure 6D, E). Correlatively, while injection of CDYL-shRNA in the PL alleviated CSDS-induced depression-like behaviors, stereotaxically coinjecting VGF-shRNA almost completely abolished this effect (Figure 6F, G). Therefore, VGF is required for CDYL-mediated stress-induced depression.

CDYL-VGF Axis Regulates Stress-Induced Loss of Dendritic Spines

We sought to understand the underlying mechanism of CDYL-VGF axis in regulating stress-induced depression-like behaviors by examining whether this axis could affect structural plasticity in the mouse PL (29,36–39). Dendritic spine morphology analysis revealed that knockdown of VGF in the PL led to decreased density of both immature spines (stubby and thin spines) and mature spines (mushroom spines) in microdefeated mice (Figure 6H, I). In addition, we observed an enhanced miniature excitatory postsynaptic current (mEPSC) frequency in the PL pyramidal neurons incubated with VGF-derived C-terminal peptide TLQP-62 (mEPSC frequency in control cells: 0.96 ± 0.06 Hz; mEPSC frequency in TLQP-62–incubated cells: 1.46 ± 0.10 Hz; $n = 9$; $p < .01$) (Supplemental Figure S6A–C), whereas these cells exhibited similar amplitude of mEPSC recordings (mEPSC amplitude in control cells: 12.62 ± 0.51 pA; mEPSC amplitude in TLQP-62–incubated cells: 12.62 ± 0.31 pA; $n = 9$) (Supplemental Figure S6D, E). Overexpression of CDYL in the PL by AAV-CDYL injection significantly reduced the density of both immature and mature dendritic spines after microdefeat stress (Figure 7A, B). Importantly, while injection of shRNA-CDYL viruses into the mouse PL led to increased dendritic spine density after CSDS, stereotaxically coinjecting shRNA-VGF with shRNA-CDYL almost completely abolished this effect (Figure 7C, D). Clearly, these results support that CDYL-VGF axis in the PL is important for stress-induced dendritic spine loss.

DISCUSSION

In the present study, we presented data showing that histone Kcr, a recently identified histone PTM, is downregulated in the mPFC of susceptible rodents exposed to CSDS. We demonstrated that the key mediator to regulate histone Kcr in the mPFC upon CSDS is CDYL, a crotonyl-CoA hydratase that we recently identified to negatively regulate histone Kcr (21). CDYL promotes stress-induced depression mainly through its dual effect on promoter histone Kcr and H3K27me3 to inhibit the transcription of a cohort of genes including VGF (Figure 7E). The CDYL-VGF axis then inhibits structural synaptic plasticity in the mPFC and ultimately leads to behavior changes in susceptible individuals (Figure 7E).

Figure 6. The chromodomain Y-like protein (CDYL)–VGF nerve growth factor inducible (VGF) pathway regulates stress-induced depression-like behaviors. **(A)** Real-time polymerase chain reaction (PCR) assays (left) and Western blotting (middle) showing that VGF was significantly reduced after VGF-short hairpin RNA (shRNA) lentivirus injection into the mouse prelimbic cortex (PL) area for 14 days, and quantification was done by normalizing the level of VGF to that of β-actin (right). $n = 4$, one-way analysis of variance (ANOVA) with Bonferroni's test, $^*p < .05$. Knockdown of VGF in the mouse PL decreased **(B)** social interaction (SI) ratio and **(C)** sucrose preference (SP) after microdefeat stress when compared with the control mice. $n = 16$–17, one-way ANOVA with Bonferroni's test, $^*p < .05$. **(D)** Expression of lentiviruses containing shRNA-CDYL and shRNA-VGF 14 days after injection into the mouse PL area. Scale bar = 0.2 mm (left), 35 μm (right). **(E)** Western blotting showing that infection of shRNA-VGF lentiviruses could counteract the upregulation of VGF induced by knockdown of CDYL (left). Quantification was done by normalizing the level of VGF to that of β-actin (right). $n = 3$, one-way ANOVA with Bonferroni's test, $^*p < .05$. Knockdown of VGF reversed the increased **(F)** SI ratio and **(G)** SP caused by knockdown of CDYL in the mouse PL after chronic social defeat stress. $n = 8$–9, one-way ANOVA with Bonferroni's test, $^*p < .05$. **(H)** Representative confocal z-stack images of a neurobiotin-filled PL pyramidal cell (left) and selected dendritic segments (right). The dendritic segments from mice injected shRNA-VGF or shRNA-control lentiviruses after microdefeat stress. Yellow arrows indicate stubby spines, white arrows indicate thin spines and blue arrows indicate mushroom spines. Scale bar = 25 μm (left), 1 μm (right). **(I)** Knockdown of VGF significantly reduced stubby, thin, mushroom, or total number of dendritic spines in mouse PL pyramidal cells after microdefeat stress. $n = 40$ neurons from 4 mice per group. Unpaired two-tailed Student's t test, $^*p < .05$, $^{**}p < .01$. Data are presented as mean ± SEM. mRNA, messenger RNA.

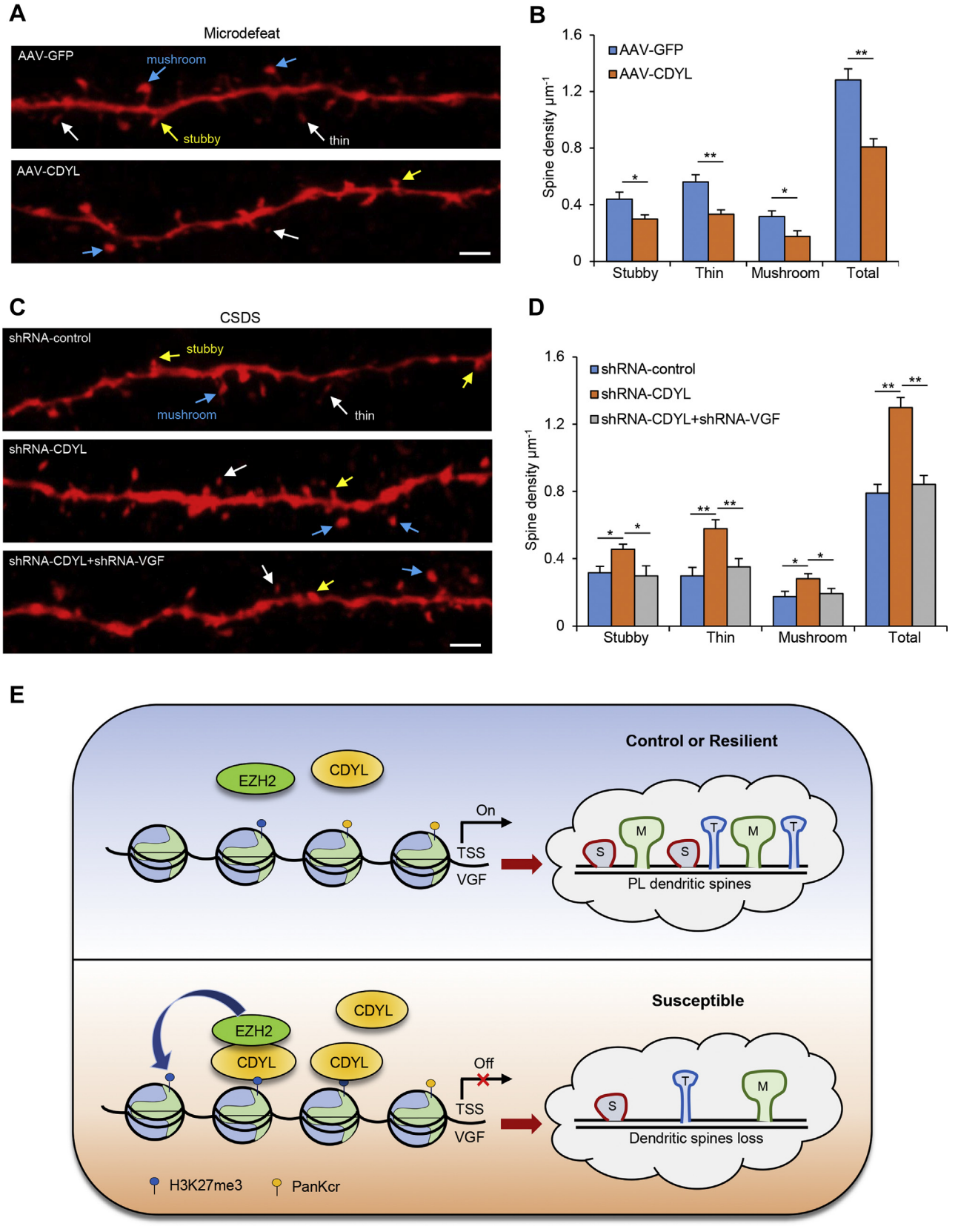
A
Microdefeat
AAV-GFP
mushroom
stubby
thin
AAV-CDYL
B
AAV-GFP
AAV-CDYL
Spine density μm-1
1.6
1.2
0.8
0.4
0
Stubby
Thin
Mushroom
Total
C
CSDS
shRNA-control
stubby
mushroom
thin
shRNA-CDYL
shRNA-CDYL+shRNA-VGF
D
shRNA-control
shRNA-CDYL
shRNA-CDYL+shRNA-VGF
Spine density μm-1
Stubby
Thin
Mushroom
Total
E
Control or Resilient
EZH2
CDYL
On
TSS
VGF
PL dendritic spines
Susceptible
Off
Dendritic spines loss
H3K27me3
PanKcr

The role of epigenetic mechanism in mediating stress-induced depression has been actively investigated in recent years (4,5). Studies have shown that adenosine triphosphate–dependent chromatin assembly factor chromatin-remodeling complex (31) and DNA methyltransferase Dnmt3a (40) are upregulated in the NAc in social stress–induced depression, while H3K9 methyltransferase G9a is decreased in the NAc during cocaine-induced depression (41). Moreover, dysregulated expression of HDACs has been found in peripheral white blood cells of MDD patients or different brain regions such as hippocampus or amygdala in rodents with stress-induced depression (42,43). While some studies suggest that HDAC inhibitors have promising antidepressant effect in animal models, their application in human patients is limited owing to low isoform selectivity, and thus the risk of serious adverse events (44,45). In this study, we found that histone Kcr, a novel type of histone acylations, is selectively downregulated in the PL during CSDS-induced depression. Noticeably, in our system we detected concomitant upregulation of crotonyl-CoA hydratase CDYL but not of other Kcr-regulating enzymes such as p300 and HDACs, suggesting that CDYL plays a major role in mediating stress-induced alteration of histone Kcr in the PL. Our finding is intriguing, as it provides the first clue regarding how dysregulation of novel types of histone acylations could play a role in environmentally influenced neuropsychological diseases such as depression. As the donors of histone acylations often come from intermediate metabolism, which dynamically responds to extracellular and intracellular stimuli in different cell types, it will be interesting to further study the functional connection between histone acylations and other types of brain disorders.

The structural and functional plasticity of dendritic spines plays an essential role in experience-dependent reorganization of the brain neural networks, which store and maintain the information in individual synapses, neurons, and neuronal circuits to guide the behavior of the organism (46,47). In the process of learning and memory, the increased functional plasticity is tightly correlated with the alteration in the number, size, and morphology of dendritic spines (48). For example, contextual fear conditioning leads to an increase in the density of dendritic spines in the hippocampal CA1 and the anterior cingulate cortex (49–51). Although these mechanisms allow the organism to adapt to its constantly evolving environment, under prolonged bouts of physiological and psychological stress, the mechanism of structural or functional plasticity may become dysregulated and the connectivity between the brain regions may become unbalanced, resulting in pathological behaviors. For instance, chronic stress significantly reduced the number of dendritic spines in the PFC (25) and induced the formation of stubby excitatory spines through a RAS-related C3 botulinum toxin substrate 1–dependent mechanism in the NAc (24). These data suggest that extracellular stimuli and environmental events robustly regulate neuronal network through altering structural plasticity, resulting in the development of depression. However, so far it is still not clear how the chronic stress or unusual synaptic activities lead to the abnormal structural plasticity. In our study, we have shown that CSDS results in significantly increased expression of CDYL in the mPFC, consequently leading to decreased expression of VGF. We also demonstrated CDYL-VGF axis regulates the structural plasticity of dendritic spines during stress-induced depression. As an activity-dependent epigenetic factor, CDYL expression is regulated by the activation of *N*-methyl-D-aspartate receptors (20). Therefore, we speculate that CDYL could be an essential mediator linking synaptic activities and long-term structural plasticity of synaptic spines. Under physiological conditions, activation of *N*-methyl-D-aspartate receptors finely regulates long-term structural plasticity via the CDYL-VGF axis. However, unusual synaptic activities in the PL induced by chronic stress may abnormally activate *N*-methyl-D-aspartate receptors and send inappropriate signals from synapses to the nuclear transcription apparatus, which in turn leads to a dysregulated CDYL-VGF axis, reduced dendritic spines, and ultimately, the development of depression.

VGF encodes a secreted protein and neuropeptide precursor that is abundantly present in the cortex, hypothalamus, hippocampus, cerebellum, and other brain areas with various concentrations (52). The role of VGF in depression has been supported by several previous studies. For example, heterozygous *Vgf* KO mice exhibit depression-like phenotypes (32), and intrahippocampal administration of VGF-derived peptide TLQP-62 produces antidepressant effects (53). Despite the important role of VGF in depression and many other physiological/pathological conditions, the transcriptional regulation of this gene is not fully understood. Previous microarray data have shown that transcription factor neuronal PAS domain protein 3 positively regulates VGF in human embryonic kidney 293 cells (54), whereas REST inhibits VGF expression in human neuroblastoma NMB cells (55). Here we demonstrate that CDYL inhibits VGF expression in mouse PL tissues and SH-SY5Y cells via its dual effect on histone Kcr and H3K27me3 on the gene promoter, providing the epigenetic mechanism for transcriptional repression of VGF. Interestingly, a recent study suggested that CSDS leads to elevated VGF protein levels in the NAc and that overexpression of *Vgf* in the NAc is prodepressant (53). We found that injection of CDYL-shRNA lentiviruses in NAc led to upregulation of VGF and increased social avoidance behavior upon microdefeat, and that this effect was

Figure 7. Chromodomain Y-like protein (CDYL) promotes stress-induced loss of dendritic spines in the mouse prelimbic cortex (PL). **(A)** Representative 63× confocal z-stack images of dendrite segments of PL pyramidal cells from mice injected with adeno-associated virus–green fluorescent protein (AAV-GFP) or AAV-CDYL after microdefeat stress. Yellow arrows indicate stubby spines, white arrows indicate thin spines, and blue arrows indicate mushroom spines. Scale bar = 1 μm. **(B)** Overexpression of CDYL significantly reduced stubby, thin, mushroom, or total number of dendritic spines in the PL after microdefeat stress. $n = 45$ neurons from 4 mice per group, unpaired two-tailed Student's t test, $^{*}p < .05$, $^{**}p < .01$. **(C)** Representative 63× confocal z-stack images of dendrite segments of PL pyramidal cells from mice injected short hairpin RNA (shRNA)–control, shRNA-CDYL, or both shRNA-CDYL and shRNA–VGF nerve growth factor inducible (VGF) lentiviruses after chronic social defeat stress (CSDS). Scale bar = 1 μm. **(D)** CDYL promoted stress-induced loss of dendritic spines mainly through inhibiting VGF expression. $n = 40$ neurons from 4 mice per group, one-way analysis of variance with Bonferroni's test, $^{*}p < .05$, $^{**}p < .01$. **(E)** Proposed model of the CDYL-VGF axis in mediating stress-induced depression-like behaviors. Data are presented as mean ± SEM. M, mushroom spine; S, stubby spine; T, thin spine; TSS, transcription start site.

abolished by coinjection of VGF-shRNA (Supplemental Figure S7). However, we do not consider that the CDYL-VGF axis in the NAc plays a major role during naturally occurring stress-induced depression, because both CDYL and the mRNA level of *Vgf* are unchanged in the NAc after CSDS in susceptible mice (53) (Supplemental Figure S2A). The alteration of VGF protein levels in the NAc after CSDS could be due to PTMs such as reduced protein degradation by the ubiquitin-proteasome pathway. It is also interesting to note that brain-derived neurotrophic factor has been known to induce VGF expression and play a role in VGF-mediated antidepressant effects (36,53,56). While the current study clearly shows that the CDYL-VGF axis in the PL is critical in regulating structural synaptic plasticity and depression, we cannot exclude that brain-derived neurotrophic factor plays a role in CDYL-mediated effect on stress-induced depression, as we have previously shown that CDYL also represses brain-derived neurotrophic factor expression (18). Nevertheless, the establishment of CDYL in mediating increased vulnerability to stress-induced depression-like behaviors provides a novel therapeutic target for MDD, especially considering that CDYL possesses a defined chromodomain and catalytic domain for design of small molecule inhibitors.

ACKNOWLEDGMENTS AND DISCLOSURES

This work was supported by the Ministry of Science and Technology of China Grant Nos. 2017YZ0072839 (to ZH) and 2015CB559200 (to ZH); National Natural Science Foundation of China Grant Nos. 31871083 (to ZH), 81371432 (to ZH), 81572771 (to JL), 91219201 (to YS), and 81130048 (to YS); Beijing Natural Science Foundation (Grant No. 7182087 to ZH); and the Innovative Fund for Doctoral Students (to YL) from Peking University Health Science Center.

YL performed and analyzed RNA sequencing, chromatin immunoprecipitation quantitative polymerase chain reaction, Western blotting, spine analysis and immunostaining. ML performed and analyzed virus microinjection, open field test, social defeat stress and chronic unpredictable mild stress. MF performed patch-clamp recordings. YS helped with Western blot experiments. HY characterized *Cdyl* transgenic mice. XZ helped with chronic social defeat stress. KX, SL, JZ, and XJ helped with patch-clamp recording. ZH, YL, and JL designed the experiments, JL, ZH, YL, ML, and YS wrote the article.

The authors report no biomedical financial interests or potential conflicts of interest.

ARTICLE INFORMATION

From the State Key Laboratory of Natural and Biomimetic Drugs (YL, ML, MF, YS, XZ, KX, SL, JZ, XJ, ZH), Department of Molecular and Cellular Pharmacology, School of Pharmaceutical Sciences, and Key Laboratory of Carcinogenesis and Translational Research (Ministry of Education) (YL, HY, YS, JL), Department of Biochemistry and Molecular Biology, School of Basic Medical Sciences, Peking University Health Science Center; Department of Biochemistry and Molecular Biology (YS), School of Basic Medical Sciences, Capital Medical University; and the Key Laboratory for Neuroscience (ZH), Ministry of Education and National Health Commission, Beijing, China.

YL and ML contributed equally to this work.

Address correspondence to Jing Liang, Ph.D., Department of Biochemistry and Molecular Biology, Peking University Health Science Center, 38 Xue Yuan Road, Beijing 100191, China; E-mail: liang_jing@bjmu.edu.cn; or Zhuo Huang, Ph.D., Department of Molecular and Cellular Pharmacology, Peking University Health Science Center, 38 Xue Yuan Road, Beijing 100191, China; E-mail: huangz@hsc.pku.edu.cn.

Received Jul 18, 2018; revised Nov 12, 2018; accepted Nov 29, 2018.

Supplementary material cited in this article is available online at https://doi.org/10.1016/j.biopsych.2018.11.025.

REFERENCES

1. Kessler RC, Berglund P, Demler O, Jin R, Koretz D, Merikangas KR, *et al.* (2003): The epidemiology of major depressive disorder: Results from the National Comorbidity Survey Replication (NCS-R). JAMA 289:3095–3105.
2. Krishnan V, Nestler EJ (2008): The molecular neurobiology of depression. Nature 455:894–902.
3. Russo SJ, Nestler EJ (2013): The brain reward circuitry in mood disorders. Nat Rev Neurosci 14:609–625.
4. Nestler EJ, Pena CJ, Kundakovic M, Mitchell A, Akbarian S (2016): Epigenetic basis of mental illness. Neuroscientist 22:447–463.
5. Nestler EJ (2014): Epigenetic mechanisms of depression. JAMA Psychiatry 71:454–456.
6. Chen Y, Sprung R, Tang Y, Ball H, Sangras B, Kim SC, *et al.* (2007): Lysine propionylation and butyrylation are novel post-translational modifications in histones. Mol Cell Proteomics 6:812–819.
7. Peng C, Lu Z, Xie Z, Cheng Z, Chen Y, Tan M, *et al.* (2011): The first identification of lysine malonylation substrates and its regulatory enzyme. Mol Cell Proteomics 10:M111.012658.
8. Tan M, Luo H, Lee S, Jin F, Yang JS, Montellier E, *et al.* (2011): Identification of 67 histone marks and histone lysine crotonylation as a new type of histone modification. Cell 146:1016–1028.
9. Dai L, Peng C, Montellier E, Lu Z, Chen Y, Ishii H, *et al.* (2014): Lysine 2-hydroxyisobutyrylation is a widely distributed active histone mark. Nat Chem Biol 10:365–370.
10. Xie Z, Zhang D, Chung D, Tang Z, Huang H, Dai L, *et al.* (2016): Metabolic regulation of gene expression by histone lysine beta-hydroxybutyrylation. Mol Cell 62:194–206.
11. Sabari BR, Tang Z, Huang H, Yong-Gonzalez V, Molina H, Kong HE, *et al.* (2015): Intracellular crotonyl-CoA stimulates transcription through p300-catalyzed histone crotonylation. Mol Cell 58:203–215.
12. Bao X, Wang Y, Li X, Li XM, Liu Z, Yang T, *et al.* (2014): Identification of 'erasers' for lysine crotonylated histone marks using a chemical proteomics approach. Elife 3:02999.
13. Feldman JL, Baeza J, Denu JM (2013): Activation of the protein deacetylase SIRT6 by long-chain fatty acids and widespread deacylation by mammalian sirtuins. J Biol Chem 288:31350–31356.
14. Fellows R, Denizot J, Stellato C, Cuomo A, Jain P, Stoyanova E, *et al.* (2018): Microbiota derived short chain fatty acids promote histone crotonylation in the colon through histone deacetylases. Nat Commun 9:105.
15. Zhao D, Guan H, Zhao S, Mi W, Wen H, Li Y, *et al.* (2016): YEATS2 is a selective histone crotonylation reader. Cell Res 26:629–632.
16. Li Y, Sabari BR, Panchenko T, Wen H, Zhao D, Guan H, *et al.* (2016): Molecular coupling of histone crotonylation and active transcription by AF9 YEATS domain. Mol Cell 62:181–193.
17. Zhang Y, Yang X, Gui B, Xie G, Zhang D, Shang Y, *et al.* (2011): Corepressor protein CDYL functions as a molecular bridge between polycomb repressor complex 2 and repressive chromatin mark trimethylated histone lysine 27. J Biol Chem 286:42414–42425.
18. Qi C, Liu S, Qin R, Zhang Y, Wang G, Shang Y, *et al.* (2014): Coordinated regulation of dendrite arborization by epigenetic factors CDYL and EZH2. J Neurosci 34:4494–4508.
19. Li X, Liang J, Yu H, Su B, Xiao C, Shang Y, *et al.* (2007): Functional consequences of new exon acquisition in mammalian chromodomain Y-like (CDYL) genes. Trends Genet 23:427–431.
20. Liu Y, Lai S, Ma W, Ke W, Zhang C, Liu S, *et al.* (2017): CDYL suppresses epileptogenesis in mice through repression of axonal Nav1.6 sodium channel expression. Nat Commun 8:355.
21. Liu S, Yu H, Liu Y, Liu X, Zhang Y, Bu C, *et al.* (2017): Chromodomain protein CDYL acts as a crotonyl-CoA hydratase to regulate histone crotonylation and spermatogenesis. Mol Cell 67:853–866 e855.
22. Golden SA, Covington HE 3rd, Berton O, Russo SJ (2011): A standardized protocol for repeated social defeat stress in mice. Nat Protoc 6:1183–1191.
23. Krishnan V, Han MH, Graham DL, Berton O, Renthal W, Russo SJ, *et al.* (2007): Molecular adaptations underlying susceptibility and resistance to social defeat in brain reward regions. Cell 131:391–404.
24. Golden SA, Christoffel DJ, Heshmati M, Hodes GE, Magida J, Davis K, *et al.* (2013): Epigenetic regulation of RAC1 induces

synaptic remodeling in stress disorders and depression. Nat Med 19:337–344.
25. Ota KT, Liu RJ, Voleti B, Maldonado-Aviles JG, Duric V, Iwata M, *et al.* (2014): REDD1 is essential for stress-induced synaptic loss and depressive behavior. Nat Med 20:531–535.
26. Kim CS, Brager DH, Johnston D (2018): Perisomatic changes in h-channels regulate depressive behaviors following chronic unpredictable stress. Mol Psychiatry 23:892–903.
27. Liu Y, Liu S, Yuan S, Yu H, Zhang Y, Yang X, *et al.* (2017): Chromodomain protein CDYL is required for transmission/restoration of repressive histone marks. J Mol Cell Biol 9:178–194.
28. Carlen M (2017): What constitutes the prefrontal cortex? Science 358:478–482.
29. Kang HJ, Voleti B, Hajszan T, Rajkowska G, Stockmeier CA, Licznerski P, *et al.* (2012): Decreased expression of synapse-related genes and loss of synapses in major depressive disorder. Nat Med 18:1413–1417.
30. Wohleb ES, Franklin T, Iwata M, Duman RS (2016): Integrating neuroimmune systems in the neurobiology of depression. Nat Rev Neurosci 17:497–511.
31. Sun H, Damez-Werno DM, Scobie KN, Shao NY, Dias C, Rabkin J, *et al.* (2015): ACF chromatin-remodeling complex mediates stress-induced depressive-like behavior. Nat Med 21:1146–1153.
32. Hunsberger JG, Newton SS, Bennett AH, Duman CH, Russell DS, Salton SR, *et al.* (2007): Antidepressant actions of the exercise-regulated gene VGF. Nat Med 13:1476–1482.
33. Cattaneo A, Sesta A, Calabrese F, Nielsen G, Riva MA, Gennarelli M (2010): The expression of VGF is reduced in leukocytes of depressed patients and it is restored by effective antidepressant treatment. Neuropsychopharmacology 35:1423–1428.
34. Jiang H, Chen S, Lu N, Yue Y, Yin Y, Zhang Y, *et al.* (2017): Reduced serum VGF levels were reversed by antidepressant treatment in depressed patients. World J Biol Psychiatry 18:586–591.
35. Ramos A, Rodriguez-Seoane C, Rosa I, Trossbach SV, Ortega-Alonso A, Tomppo L, *et al.* (2014): Neuropeptide precursor VGF is genetically associated with social anhedonia and underrepresented in the brain of major mental illness: Its downregulation by DISC1. Hum Mol Genet 23:5859–5865.
36. Alder J, Thakker-Varia S, Bangasser DA, Kuroiwa M, Plummer MR, Shors TJ, *et al.* (2003): Brain-derived neurotrophic factor-induced gene expression reveals novel actions of VGF in hippocampal synaptic plasticity. J Neurosci 23:10800–10808.
37. Thakker-Varia S, Alder J (2009): Neuropeptides in depression: Role of VGF. Behav Brain Res 197:262–278.
38. Behnke J, Cheedalla A, Bhatt V, Bhat M, Teng S, Palmieri A, *et al.* (2017): Neuropeptide VGF Promotes Maturation of Hippocampal Dendrites That Is Reduced by Single Nucleotide Polymorphisms. Int J Mol Sci 18:E612.
39. Duman RS, Aghajanian GK (2012): Synaptic dysfunction in depression: Potential therapeutic targets. Science 338:68–72.
40. LaPlant Q, Vialou V, Covington HE 3rd, Dumitriu D, Feng J, Warren BL, *et al.* (2010): Dnmt3a regulates emotional behavior and spine plasticity in the nucleus accumbens. Nat Neurosci 13:1137–1143.
41. Covington HE 3rd, Maze I, Sun H, Bomze HM, DeMaio KD, Wu EY, *et al.* (2011): A role for repressive histone methylation in cocaine-induced vulnerability to stress. Neuron 71:656–670.
42. Pena CJ, Bagot RC, Labonte B, Nestler EJ (2014): Epigenetic signaling in psychiatric disorders. J Mol Biol 426:3389–3412.
43. Covington HE 3rd, Vialou VF, LaPlant Q, Ohnishi YN, Nestler EJ (2011): Hippocampal-dependent antidepressant-like activity of histone deacetylase inhibition. Neurosci Lett 493:122–126.
44. Covington HE 3rd, Maze I, LaPlant QC, Vialou VF, Ohnishi YN, Berton O, *et al.* (2009): Antidepressant actions of histone deacetylase inhibitors. J Neurosci 29:11451–11460.
45. Misztak P, Panczyszyn-Trzewik P, Sowa-Kucma M (2018): Histone deacetylases (HDACs) as therapeutic target for depressive disorders. Pharmacol Rep 70:398–408.
46. Christoffel DJ, Golden SA, Russo SJ (2011): Structural and synaptic plasticity in stress-related disorders. Rev Neurosci 22:535–549.
47. Holtmaat A, Svoboda K (2009): Experience-dependent structural synaptic plasticity in the mammalian brain. Nat Rev Neurosci 10:647–658.
48. Yoshihara Y, De Roo M, Muller D (2009): Dendritic spine formation and stabilization. Curr Opin Neurobiol 19:146–153.
49. Restivo L, Vetere G, Bontempi B, Ammassari-Teule M (2009): The formation of recent and remote memory is associated with time-dependent formation of dendritic spines in the hippocampus and anterior cingulate cortex. J Neurosci 29:8206–8214.
50. Vetere G, Restivo L, Cole CJ, Ross PJ, Ammassari-Teule M, Josselyn SA, *et al.* (2011): Spine growth in the anterior cingulate cortex is necessary for the consolidation of contextual fear memory. Proc Natl Acad Sci U S A 108:8456–8460.
51. Basu S, Lamprecht R (2018): The role of actin cytoskeleton in dendritic spines in the maintenance of long-term memory. Front Mol Neurosci 11:143.
52. Salton SR, Ferri GL, Hahm S, Snyder SE, Wilson AJ, Possenti R, *et al.* (2000): VGF: A novel role for this neuronal and neuroendocrine polypeptide in the regulation of energy balance. Front Neuroendocrinol 21:199–219.
53. Jiang C, Lin WJ, Sadahiro M, Labonte B, Menard C, Pfau ML, *et al.* (2018): VGF function in depression and antidepressant efficacy. Mol Psychiatry 23:1632–1642.
54. Sha L, MacIntyre L, Machell JA, Kelly MP, Porteous DJ, Brandon NJ, *et al.* (2012): Transcriptional regulation of neurodevelopmental and metabolic pathways by NPAS3. Mol Psychiatry 17:267–279.
55. Moon SM, Kim JS, Park BR, Kim DK, Kim SG, Kim HJ, *et al.* (2015): Transcriptional regulation of the neuropeptide VGF by the neuron-restrictive silencer factor/neuron-restrictive silencer element. Neuroreport 26:144–151.
56. Lin P, Wang C, Xu B, Gao S, Guo J, Zhao X, *et al.* (2014): The VGF-derived peptide TLQP62 produces antidepressant-like effects in mice via the BDNF/TrkB/CREB signaling pathway. Pharmacol Biochem Behav 120:140–148.